Photosynth Res (2007) 92:55–63
DOI 10.1007/s11120-006-9125-1

REGULAR PAPER

Two equilibration pools of chlorophylls in the Photosystem I core antenna of *Chlamydomonas reinhardtii*

Krzysztof Gibasiewicz · V. M. Ramesh · Su Lin · Kevin Redding · Neal W. Woodbury · Andrew N. Webber

Received: 2 June 2006 / Accepted: 11 December 2006 / Published online: 5 July 2007

Summary Femtosecond transient absorption spectroscopy was applied for a comparative study of excitation decay in several different Photosystem I (PSI) core preparations from the green alga *Chlamydomonas reinhardtii*. For PSI cores with a fully interconnected network of chlorophylls, the excitation energy was equilibrated over a pool of chlorophylls absorbing at ~683 nm, independent of excitation wavelength [Gibasiewicz et al. J Phys Chem B 105:11498–11506, 2001; J Phys Chem B 106:6322–6330, 2002]. In preparations with impaired connectivity between chlorophylls, we have found that the spectrum of chlorophylls connected to the reaction center (*i.e.*, with ~20 ps decay time) over which the excitation is equilibrated becomes excitation-wavelength-dependent. Excitation at 670 nm is finally equilibrated over chlorophylls absorbing at ~675 nm, whereas excitation at 695 nm or 700 nm is equilibrated over chlorophylls absorbing at ~683 nm. This indicates that in the vicinity of the reaction center there are two spectrally different and spatially separated pools of chlorophylls that are equally capable of effective excitation energy transfer to the reaction center. We propose that they are related to the two groups of central PSI core chlorophylls lying on the opposite sides of reaction center.

Keywords Antenna · Chlorophylls · Excitation energy transfer · Femtosecond transient absorption · Photosystem I · Primary charge separation · Reaction center

Abbreviations

A_0	Primary acceptor
A_1	Secondary quinone acceptor
Chl	Chlorophyll
DADS	Decay associated difference spectrum
ND	Non-decaying
P700	Primary donor
PB	Photobleaching
PSI	Photosystem I
RC	Reaction center
SE	Stimulated emission

K. Gibasiewicz · V. M. Ramesh · A. N. Webber
School of Life Sciences, Department of Chemistry and Biochemistry and Center for the Study of Early Events in Photosynthesis, Arizona State University, Tempe AZ 85287-4501, USA

S. Lin · N. W. Woodbury
Department of Chemistry and Biochemistry, Arizona State University, Tempe, AZ 85287-4501, USA

K. Gibasiewicz · V. M. Ramesh · S. Lin · N. W. Woodbury · A. N. Webber
Center for the Study of Early Events in Photosynthesis, Arizona State University, Tempe, AZ 85287-4501, USA

K. Gibasiewicz (✉)
Department of Physics, Adam Mickiewicz University, ul. Umultowska 85, 61-614 Poznan, Poland
e-mail: krzyszgi@amu.edu.pl

K. Redding
Department of Chemistry, University of Alabama, Box 870336, Tuscaloosa, AL 35487-0336, USA

Introduction

A high resolution structure of the PSI core (2.5 Å) from the cyanobacterium *Thermosynechococcus elongatus* (Jordan

et. al 2001; Fromme et al. 2001) allows identification of ninety antenna chlorophylls (Chls) and six reaction center (RC) Chls. Seventy nine antenna Chls are bound by the central PsaA and PsaB subunits, and eleven Chls are bound by a few peripheral subunits of the PSI core complex. Both PsaA and PsaB contain 11 transmembrane α-helices. Two Chls, called connecting Chls, have a special location between the antenna and the RC, and have been proposed to form a major route of excitation energy flow between these two compartments (Jordan et al. 2001). RC Chls include the dimeric primary donor, P700, two primary acceptors, A_0, and two accessory Chls, A.

Despite detailed information on the PSI core structure, the site energies of individual Chls are not known. The results from theoretical modeling provide contradictory values (Byrdin et al. 2002; Damjanović et al. 2002; Bruggemann et al. 2004). Sener et al. (2002) even concluded that exact values of particular site energies for most of Chls are not important for overall excitation dynamics in PSI. The spectral composition of the PSI core antenna Chls emerging from spectroscopic studies comprises several spectral forms of bulk Chls with Q_Y bands peaking at between ~673 (the most abundant) and ~698 nm (Melkozernov et al. 2000; Gobets et al. 1994) and a species-dependent number of red Chls absorbing at >700 nm. Several antenna Chls were shown to form dimers or trimers (Jordan et al. 2001; Byrdin et al. 2002; Damjanović et al. 2002; Sener et al. 2002), and were proposed to be the red Chls (Klug et al. 1989; Melkozernov et al. 2000a, b). No red Chls, absorbing at >700 nm, were observed in *C. reinhardtii* PSI core preparations (Gibasiewicz et al. 2001, 2002).

On the basis of femtosecond transient absorption measurements, it was suggested that within a few picoseconds after excitation of PSI core, energy is equilibrated over a small subset of relatively low-energy antenna Chls located close to the RC (Gibasiewicz et al. 2001, 2002; see also Klug et al. 1989 and Melkozernov et al. 2001). The maximum photobleaching/stimulated emission (PB/SE) signal of this pool is at ~683–685 nm (Gibasiewicz et al. 2001, 2002; Savikhin et al. 2000; Melkozernov et al. 2000a; Gobets et al. 2003) and is independent of excitation wavelength (Gibasiewicz et al. 2001).

The excitation energy transfer and trapping processes in PSI have been described by two models. The trap-limited model assumes that excitation can visit the reaction center and return to the antenna Chls many times before charge separation takes place (Melkozernov et al. 1997, 1998; Müller et al. 2003). The alternative transfer-to-the-trap-limited model (Gobets and van Grondelle 2001; Savikhin et al. 2000, 2001; Valkunas et al. 1995) assumes that equilibration of the excitation energy occurs relatively quick and the limiting step of excitation energy quenching is energy transfer from the antenna equilibrated state to the RC. Excitation, once captured by the RC, does not return to the antenna. The structural model of PSI indeed demonstrates that the antenna Chls are spatially separated from the electron transfer chain (Jordan et. al 2001; Fromme et al. 2001).

In this paper, we report an observation of two equilibration pools of Chls. In addition to the well established ~683-nm pool we observed a higher-energy pool at ~675 nm. Both these pools are well coupled to RC and are spatially separated from each other. We propose that they are related to the two groups of central PSI core Chls lying on the opposite sides of RC. In our approach, a prerequisite for the direct experimental detection of the higher-energy pool was removal of the connection between the two pools. For that purpose, we have worked with preparations showing varying amount of Chls energetically uncoupled from RC.

Materials and methods

Site-directed mutagenesis

Oligonucleotide-mediated site-directed mutagenesis was used to introduce mutations into the *psaB* gene. Four different "A_0 mutants" were obtained by replacing methionine-B664, normally coordinating A_0 in the B branch (Chl eC-B3 according to nomenclature from (Jordan et. al 2001) by histidine (MH(B664)) or serine (MS(B664)) in two different recipient strains: CC 125 and CC 2696, using protocols essentially as described previously (Ramesh et al. 2004; Lee et al. 1998; Webber et al. 1993). The strain KRC51-3A (154-1A) expresses WT PSI in a background lacking PSII and Chl *b* (Guergova-Kuras et al. 2001).

Preparation of PSI particles

PSI particles were prepared as described earlier (Gibasiewicz et al. 2001; Krabben et al. 2000). They have been prepared from two different "wild type" strains and four mutants described above. The "wild type" strains, CC 2696 and KRC51-3A (154-1A), are devoid of LHCI and PSII, as demonstrated by lack/negligible amount of steady state absorption from Chl *b* (Fig. 1), but have normal PSI core. As shown in the Results section, PSI preparations from all these different strains are characterized by different amounts of Chls that are energetically uncoupled to the RC. The differences in the relative amounts of uncoupled Chls between all these preparations are thought to be due to differences in temperature and light intensity during growth, due to differences in vulnerability of the

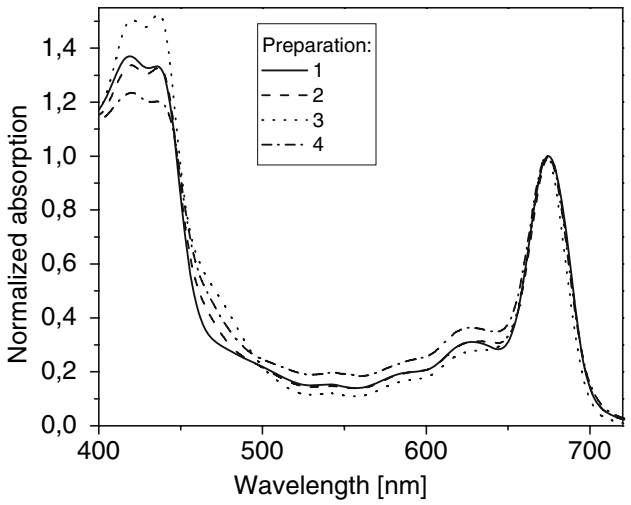

Fig. 1 Comparison of the steady-state absorption spectra of four PSI preparations covering the whole presented range of uncoupled Chls (from ~0% of uncoupled Chls for preparation 1 to ~60% - for preparation 4)

mutants to the preparation procedure, and/or to slight differences in the preparation procedures. Throughout the text, the following marking numbers are assigned to particular PSI core preparations: (1) KRC51-3A (154-1A) WT, (2) CC2696 WT, (3) another preparation of KRC51-3A (154-1A) WT, (4) MS(B664) in CC 2696, (5) MS(B664) in CC 125, (6) MH(B664) in CC 125, (7) MH(B664) in CC 2696.

Femtosecond transient absorption measurements were described earlier (Gibasiewicz et al. 2001, 2002; Freiberg et al. 1998). Selective excitation of different spectral subpopulations of antenna Chls was realized by applying 5-nm wide (fwhm) ~150-fs pulses centered at 670, 680, 695, 700, 705 and 710 nm. The transient spectra were typically measured between 600 and 750 nm on two time scales: from –1 ps to ~5 ps with a step size of 54 fs and from 5 ps to 100 ps with a step size of 2 ps. The spectral resolution of the presented data is 2 nm. 20 mM sodium ascorbate and 10 μM phenazine methosulfate were added to the samples to ensure efficient rereduction of the oxidized primary donor after each excitation pulse. Excitation energies were kept on the low level of less than 1 photon per RC to avoid annihilation effects. The temporal evolution of transient spectra was analyzed globally yielding decay-associated difference spectra, DADS (see e.g. (van Stokkum et al. 2004) for theory).

Millisecond transient absorption measurements

The instrument was previously described in (Kleinherenbrink et al. 1994).

Interaction energies

Interaction energies between i-th and j-th Chls, V_{ij}, were calculated according to the dipole–dipole interaction formula (van Amerongen et al. 2000):

$$Vij = 5.04C\mu^2\kappa_{ij}/R_{ij}^3, \quad (1)$$

where the orientation factor κ_{ij} is defined as

$$\kappa_{ij} = \boldsymbol{\mu}_i \cdot \boldsymbol{\mu}_j - 3(\boldsymbol{\mu}_i \cdot \boldsymbol{R}_{ij})(\boldsymbol{\mu}_j \cdot \boldsymbol{R}_{ij}), \quad (2)$$

μ^2 is the dipole strength of Chl a, C is a constant dependent on the dielectric constant of the medium ($C\mu^2 = 19$ debye^2; Shipman 1977), R_{ij} is the center-to-center distance between the two interacting Chls, $\boldsymbol{\mu}_i$ and $\boldsymbol{\mu}_j$ are the unit vectors of their transition moments, and $\boldsymbol{R}_{ij}$ is the unit vector along the line joining centers of the respective Chls. The directions of the unit vectors and the value of R_{ij} were taken from the PSI PDB file (1JBO), assuming that the Q_Y transition moment runs through nitrogens N_B and N_D.

Results

The steady-state absorption spectra of four preparations showing different amounts of uncoupled Chls, ~0–60%, are presented in Fig. 1. Interestingly, the differences in the Q_y region are very minor, in particular between the preparations showing the lowest and the highest amounts of uncoupled Chls (prep. 1 and 4). This demonstrates that even a high amount of uncoupled Chls does not significantly affect the Chls lowest excited state distribution. In particular, no free Chls are detected, whose Q_y band is significantly blue shifted. Rather, the uncoupled Chls remain in their natural protein environment tuning their spectral properties towards the red. Some differences are observed in the blue part of the spectra, especially in the Soret/carotenoids region, showing some modifications in the protein–pigments interactions, presumably in the uncoupled parts of the PSI particles.

The dynamics of the excitation energy in all PSI core preparations was measured at a few excitation wavelengths on 100-ps time scale and analyzed globally (see, e.g., (Gibasiewicz et al. 2001)). In all the cases, two or three exponential components plus a constant or non-decaying component (ND) were necessary to obtain good fits to the experimental data. A subpiscosecond phase of 0.2–0.9 ps and a slower ~20-ps phase were always found. An additional ~2–4 ps phase was also necessary to significantly improve the fits in the case of most fittings (except for lower temporal resolution measurement on 220-ps time

scale (see below), and longer wavelength excitation at 695–700 nm (compare to Gibasiewicz et al. 2001)). The interpretation of the exponential components for all of the preparations is similar to the one given for the PSI core from CC 2696 strain of *C. reinhardtii* (Gibasiewicz et al. 2001). The two fastest phases describe energy equilibration, and the shapes of their DADS are highly excitation-wavelength-dependent in line with previous reports (Gibasiewicz et al. 2001, Melkozernov et al 2000a; Müller et al. 2003).

The ~20-ps phase is ascribed to the primary charge separation and is called the trapping component (Fig. 2A–D, Table 1). The ND component is contributed by $P700^+$ (maximum at ~691–693 nm), and by long-lived excited Chls (maximum at ~677 nm) (Fig. 2E–G). These Chls are called "uncoupled Chls" because they stayed excited much longer than ~20 ps, typical for very intact PSI cores. Figure. 2A–D compares the trapping DADS obtained for four different PSI core preparations after selective excitation of different spectral forms of antenna Chls in the range between 670 and 710 nm. In the case of preparation 2 (Fig. 2B; data were taken from (Gibasiewicz et al. 2001) for comparison), the excitation energy is finally collected by virtually the same equilibration pool of Chls centered at ~683 nm independent of the excitation wavelength (for the 670-nm excitation there is a small extra bump on the short-wavelength side of the band). Similarly, the trapping DADS for preparation 1 is relatively insensitive to excitation wavelength (Fig. 2A). Oppositely, for preparation 3, excitation at 670 nm leads to a significant blue shift and a broadening of the trapping DADS compared to those obtained for excitation at 695 and 700 nm (Fig. 2C). The effect of this blue shift is even more pronounced for preparation 4 (Fig. 2D), for which the trapping DADS for 670-nm excitation peaks at 675 nm, which is blue-shifted 8 nm compared to the DADS obtained at longer excitation wavelengths. The extent of excitation wavelength dependence of the trapping DADS is clearly correlated with the amount of uncoupled Chls (Fig. 2). An approximate measure of this dependence can be relative shift between the trapping DADS bands for shorter and longer excitation wavelength. This shift versus the amount of uncoupled Chls is presented in the upper inset in Fig. 3.

The amount of uncoupled Chls (N_{uChls}; Table 1) for each preparation and each excitation wavelength was estimated from the formula:

$$N_{uChls} = (A_{ND} - A_{P700+})/(A_{trap} + A_{ND}), \quad (3)$$

where A_{ND} is the integrated area over the ND spectrum, A_{P700+} is properly scaled area over the $P700^+$ spectrum, and A_{trap} is the area over the trapping DADS (Fig. 4). The $P700^+$ spectrum was found as the ND spectrum for preparation 1 after excitation at 695 nm (Fig. 2E; no uncoupled Chls approximation) (Melkozernov et al. 1997; Hastings et al. 1995).

The electron transfer activity in the PSI core preparations was confirmed by a transient absorption experiment performed on 100-milliseconds time scale. Samples were excited with subsaturating flashes at 532 nm and kinetic traces showing immediate formation and a slow decay of $P700^+$ were recorded at 696 nm. Figure 3 shows three kinetic traces, for preparations 1, 2, 4 (from Fig. 2), and demonstrates that the signal from $P700^+$ diminishes with the increase of the amount of Chls uncoupled from RC (see also lower inset in Fig. 3). Since all the samples were excited with the light pulses of the same energy density and the kinetic traces were normalized to the same OD, the initial amplitude of the signals is proportional to the amount of PSI particles for which the excitation reached RC and caused primary charge separation. As expected, this amount roughly linearly decreases with the increasing amount of uncoupled Chls (lower inset in Fig. 3). This correlation validates indirectly the assignment of the ~20-ps component to the photochemical quenching by charge separation.

Figure 5 shows two pairs of picosecond kinetics measured at the maxima of the two pools of Chls coupled to RC, for two preparations showing the largest amounts of uncoupled Chls (compare to Fig. 2D and upper inset in Fig. 3). For both preparations and both pools of excited Chls, the trapping kinetics is characterized by a time constant from the range 19–30 ps (see caption to Fig. 5). The kinetics collected on extended, 220-ps, time scale (Fig. 5B) demonstrates that on this time scale, the ~20-ps component is well separated from the ND component.

Discussion

The simplest and our preferred explanation for the observation of the two different trapping DADS is that there are two spectrally different equilibration pools of antenna Chls in the PSI core. Apparently, they are spatially separated, because otherwise the excitation could easily flow to the energetically lower-lying Chls with a PB/SE maximum at 683 nm. These two pools are well connected in intact preparations that contain a low amount of uncoupled Chls (Fig. 2A–B). However, when the amount of uncoupled Chls is high, the connection between these two pools is lost (Figs. 2D). There are also preparations with an intermediate quality in this connection (Fig. 2C), perhaps showing some heterogeneity: in part of the PSI cores both pools are still connected, and in part of them this connection is lost.

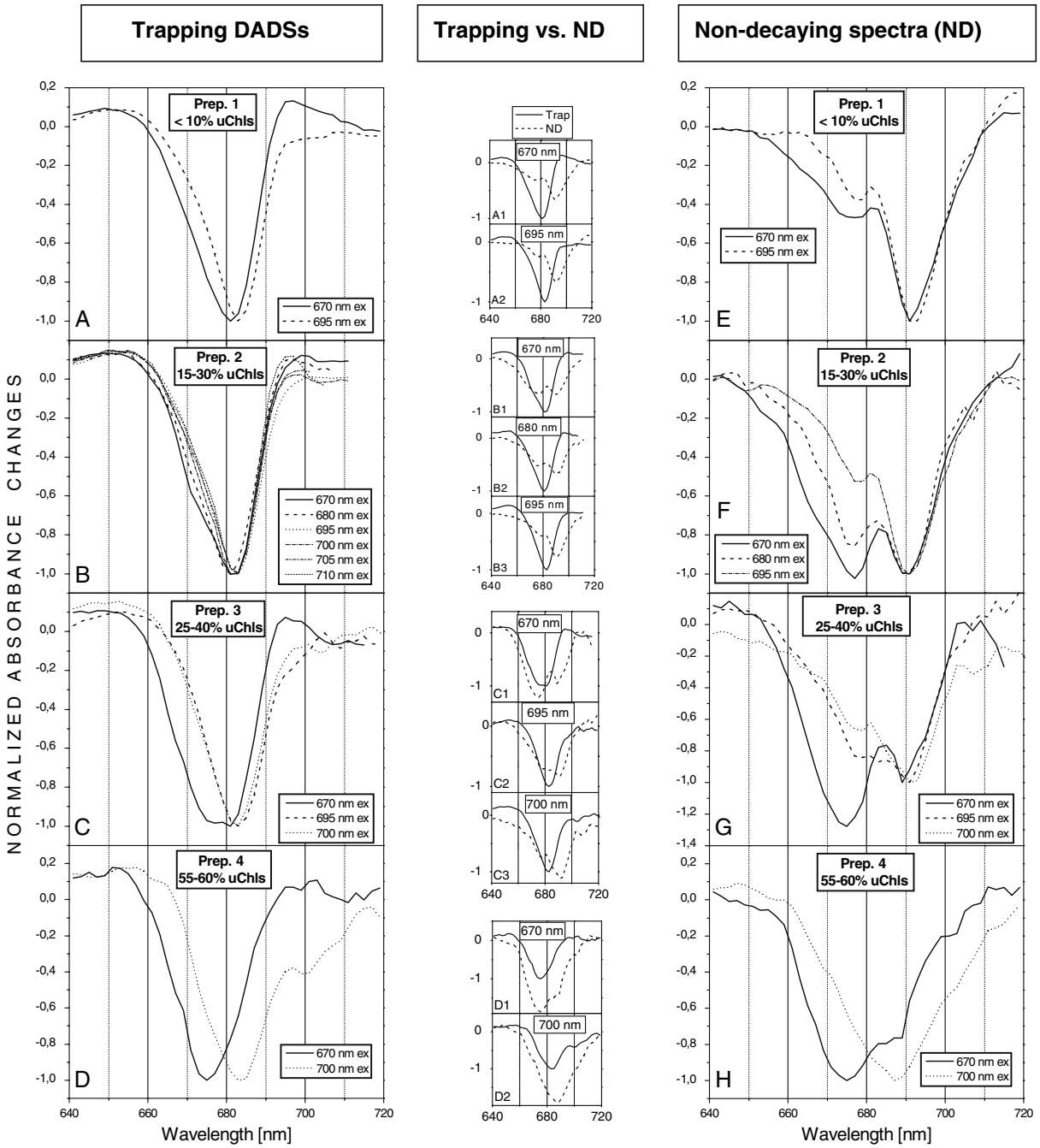

Fig. 2 Decay associated difference spectra of the trapping component and non-decaying spectra for PSI cores from four different preparations of *C. reinhardtii* (see Materials and Methods for assignment). (**A–D**) comparison of the trapping DADS normalized to the same maximal amplitude after excitation at different wavelengths. The amount of uncoupled Chls (uChls) is shown for each preparation. (**A1–D2**) comparison of the shapes and relative amplitudes of the trapping DADS and ND spectra for different excitation wavelengths for respective preparations. (**E–H**) comparison of the normalized ND spectra (normalized at 691 nm, except for (**H**), where normalization was to the same maximal amplitude)

This may be responsible for the broadening of the trapping DADS towards the blue.

An alternative explanation for the observation of the two different trapping DADS could be improper assembly of the core antenna resulting in a fraction of PSI cores without low-energy Chls forming the 683-nm pool. However, this explanation implies significant loss of the steady-state absorption at ~683 nm in preparations showing two pools, which in fact is only very minor (Fig. 1).

Table 1 Amounts of uncoupled chlorophylls (N_{uChls}) and the trapping times (τ_{trap}) found for seven different WT and mutant PSI core preparations presented in Figs. 1–3, at different excitation wavelengths (λ_{ex})

Sample		λ_{ex} [nm]	N_{uChls}·100% [%]	τ_{trap} [ps]
1	KRC51-3A (154-1A) WT A	670	9	21
		695	0	18
2	CC 2696 WT	670	28	21
		680	19	21
		695	15	21
3	KRC51-3A (154-1A) WT B	670	38	22
		695	26	19
		700	37	26
4	MS(B664) in CC 2696	670	58	19
		700	55	30
5	MS(B664) in CC 125	670	46	27
		700	20	20
6	MH(B664) in CC 125	670	43	34
		695	25	17
		700	26	12
7	MH(B664) in CC 2696	670	35	22
		700	54	19

The values of the trapping time were found from 2- or 3-component exponential fits (in addition to a non-decaying component)

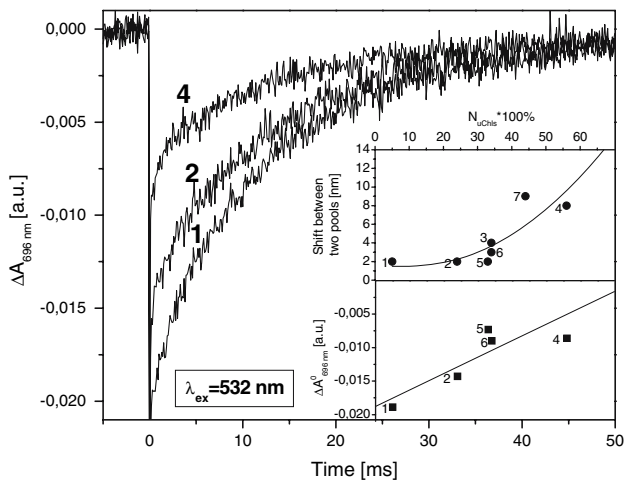

Fig. 3 Kinetic traces of absorbance changes at 696 nm due to formation and decay of $P700^+$ following a subsaturating excitation at 532 nm for three representative PSI core preparations. Lower inset: relationship between the initial amplitudes of the kinetic traces (at $t = 0$) and the fraction of Chls uncoupled from the RC in different PSI core preparations. Upper inset: shift between the absorption bands positions of the two equilibration pools vs. a fraction of Chls uncoupled from RC. 20 mM sodium ascorbate and 10 μM phenazine methosulfate was added to all samples for efficient reduction of $P700^+$. The signals were normalized to the same absorbance at the maximum of Q_y bands for all the PSI cores

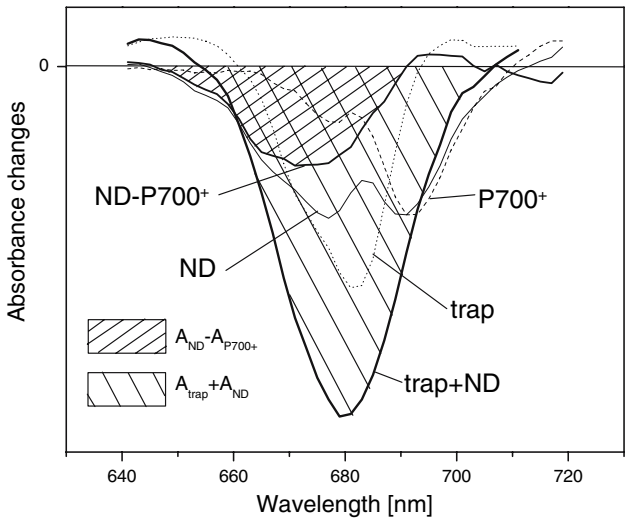

Fig. 4 Figure demonstrating how the amount of uChls has been determined from Eq. 3. Example ND and trapping DADS were taken from Fig. 2B1 (preparation 2, excitation wavelength 670 nm). Integration was performed only over the regions where the signals were negative due to PB/SE. The positive effect of ESA was assumed to be relatively low and was neglected

It is interesting to note that the trapping time of the ~675-nm pool of Chls found in the 100-ps time-scale does not deviate significantly from ~20 ps, which is the value of trapping time well established in the literature and characteristic of the ~683-nm pool (Tab. 1, Fig. 5). This indicates that the localization of both hypothetical pools is equivalent in terms of relative coupling/distance to the RC.

Structural assignments

In the following we will try to answer the question on which groups of structurally identified Chls are possible candidates for constituting the two equilibration pools, and which groups of Chls are dysfunctional in terms of transferring the excitation energy between these two pools. Since a crystal structure of PSI core from *Chlamydomonas reinhardtii* is not known we will base our considerations on the structure of PSI from cyanobacteria (Jordan et. al 2001; Fromme et al. 2001), which is expected to be very similar to that from eukaryotic organisms (Ben-Shem et al. 2003).

We propose that in the samples with high amount of uncoupled Chls, the peripheral regions of the PSI cores are somewhat removed from the central PsaA/PsaB antenna, and thus the energy transfer between the periphery and the center is broken (Fig. 6A; compare to Fig. 5C in (Jordan et. al 2001)). This seems likely because most of Chls from the peripheral antennas are bound by four PsaA and four PsaB N-terminal α-helices and adjacent loops, which are known to be

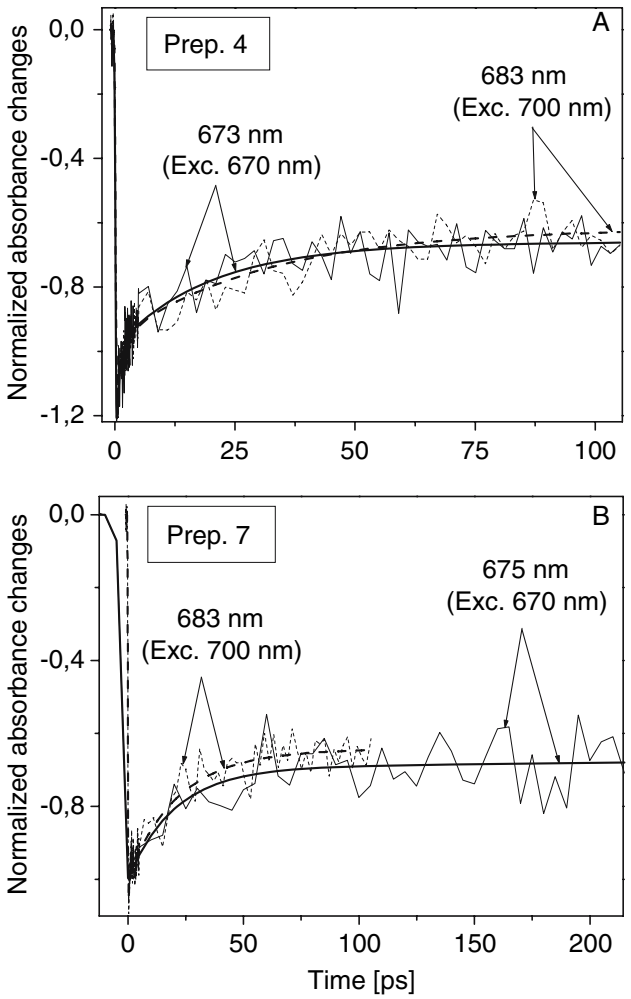

Fig. 5 Comparison of kinetics at 673 nm (675 nm) and 683 nm in preparations showing the largest amounts of uncoupled Chls (preparations 4 and 7). Thin lines represent the raw data and the thick lines—fits. The solid lines are for 670-nm excitation, and the dashed lines—for 700-nm excitation. Fits were performed with a global analysis between 630 and 720 nm and gave the following values: prep. 4 for 670-nm excitation - 0.15 ps, 0.77 ps, 19.3 ps, ND; prep. 4 for 700-nm excitation - 0.14 ps, 1.7 ps, 30 ps, ND; prep. 7 for 670-nm excitation - 22.4 ps, ND; prep. 7 for 700-nm excitation - 0.14 ps, 3.2 ps, 18.7 ps, ND. Note that the data were collected on longer, 220-ps time scale with 5-ps time step in the case of prep. 7 at 670-nm excitation in order to show that the ~20-ps component is well separated from the ND component. The normalization (multiplication of the amplitudes over a constant factor) was performed in order to directly compare the shapes of the trapping, ~20-ps, components

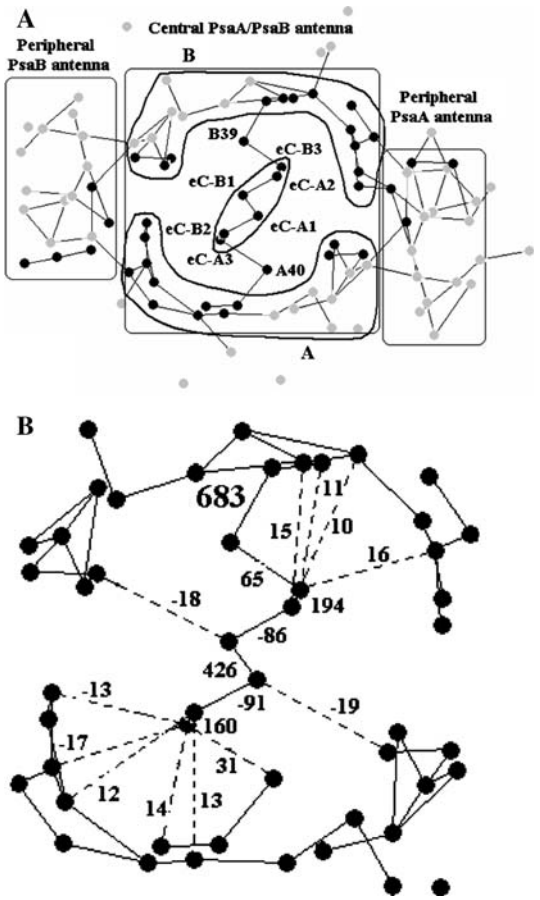

Fig. 6 Arrangement of the PSI core Chls, represented by their Mg atoms, in *Thermosynechococcus elongatus.* Solid lines join all pairs of Chls with interaction energies ≥ 30 cm^{-1}. (**A**) All 90 antenna Chls and 6 RC Chls are shown. In rectangles there are two peripheral antennas, that contain 18 Chls each, and the central antenna that contains 43 Chls in addition to the 6 RC Chls. Outside of the rectangles are 11 Chls bound by peripheral protein subunits. Chls are named after (Jordan et al. 2001). The eC-B1 and eC-A1 Chls form the primary pair P700, eC-A2 and eC-B2 are accessory Chls, and eC-B3 and eC-A3 are the primary acceptors A_0. The eC-B1, eC-A2, and eC-B3 Chls form branch B, and the remaining 3 Chls form branch A of the RC Chls. B39 and A40 are the two connecting Chls. Two groups of Chls, A and B, in central antenna are marked. In gray: Chls bound by the region of four PsaA and four PsaB N-terminal α-helices and by the peripheral subunits. In black: Chls bound by the region of seven PsaA and seven PsaB C-terminal α-helices. See text for further details. (**B**) There are shown the strongest interaction energies between the central antenna and RC Chls (dotted lines; 10–19 cm^{-1}) and between 6 RC Chls (solid lines; ≥ 50 cm^{-1})

weakly associated with the central core formed by the remaining C-terminal α-helices (Jordan et. al 2001; Fromme et al. 2001). The small PSI core subunits together with the peripheral PsaA and PsaB antennas bind slightly over 50% of the antenna Chls (47 molecules), the amount comparable with the amount of uncoupled Chls in most of our preparations showing the excitation wavelength dependence of the trapping DADS. Analysis of the distances between the Chls reveals that the peripheral PsaA and PsaB antennas bridge, from two sides, the two large Chl groups located in the central PsaA/PsaB antenna that comprise the remaining 43 antenna Chls. Twenty one Chls of one of these groups (group B in Fig. 6A) are distributed around the B branch of the electron transfer Chls, whereas 22 Chls of the other group (group A in Fig. 6A) are located around the A branch. The Mg–Mg distances between the nearest neighbors within these two

groups are in the range of 7–16 Å, whereas the distances between the closest neighbors from the two groups is above 17 Å. These distances together with mutual orientation factors allows calculation of the interaction energies between the neighboring Chls within each of these groups (>33 cm^{-1}) and between the nearest neighbors from the A and B groups (<16 cm^{-1}). The calculated values indicate separation of the two groups and suggest that in the native system, groups A and B exchange excitation energy preferentially via the peripheral PsaA and PsaB antenna (Fig. 6A). If these two peripheral antennas are separated from the center, energy exchange between the central A and B groups becomes impaired. Consequently, we propose that all or part of Chls from group A and B constitutes, respectively, the two equilibration pools reported in this paper.

There are a few indications that Chls from the group B form the lower-energy pool at ~683 nm. First, they contain two strongly interacting dimers of Chls (B37–B38 and B7–A32), whereas there is only one Chl dimer (A38–A39) in the group A with somewhat lower interaction energy (Jordan et. al 2001; Fromme et al. 2001; Byrdin et al. 2002). The excitonic interactions in dimers are expected to result in low energy states. Secondly, the B-branch connecting Chl, B39, is coupled to the RC Chl twice more strongly (65 cm^{-1}) than its A-side counterpart (31 cm^{-1}, Fig. 6B). Therefore it seems natural that concentration of the excitation energy occurs preferentially around the B-branch connecting Chls. These speculations are supported by Monte Carlo simulations of energy transfer in PSI (Byrdin et al. 2002). There was shown that the amount of energy flowing to the RC via connecting Chl B39 is twice as high as the energy flowing via its counterpart Chl A40. Also, the average site energy in the group B of Chls (Fig. 6A; 682.8 nm) is significantly lower than the average site energy in the group A (675.5 nm), supporting our postulate that energy preferentially equilibrates over Chls from group B.

As seen from Fig. 2 and Table 1 the relative amount of the excited uncoupled Chls is also excitation wavelength-dependent. In general, the largest relative amount of them is observed following excitation at 670 nm, and the longer the excitation wavelength the less uncoupled Chls were excited. If the uncoupled Chls are from peripheral regions of PSI as proposed above, this implicates a funneling arrangement of different spectral forms of Chls in PSI. Lower-energy Chls are concentrated closer to the RC than the higher energy Chls. This is in line with relatively high average site energy calculated for Chls (671.3 nm) from the peripheral antennas (Byrdin et al. 2002).

Our model implicates that excitation energy, once captured by the RC, does not return to the antenna and supports the transfer-to-the-trap-limited model. Otherwise the excitation from the ~675 nm pool could be transferred to the ~683 nm pool via the RC Chls and only the lower energy pool would have been observed independently of excitation wavelength. The increased trapping time in the case of mutated PSI cores from *C. reinhardtii* with PsaB-His656 replaced either by asparagine or phenylalanine and with increased midpoint potential of $P700/P700^+$, was interpreted in terms of the alternative trap-limited model (Melkozernov et al. 1997, 1998). However, these results do not necessary exclude that in the WT, excitation visits the RC only once, and in the mutants with unfavorable energetics for charge separation, excitation's escape from the RC to the antenna is more likely.

Our conclusion on the transfer-to-the-trap-limited model for PSI contradicts the conclusion put forward in the papers by Müller et al. (2003) and Holzwarth et al. (2005), where the opposite trap-limited model have been supported on the basis of the transient absorption experiments followed by extensive and elaborated target analysis. At the moment we are not able to indicate where a possible mistake in the cited papers could be. However, the point we would like to make is that our conclusion was based directly on very simple raw measurements, whereas the elaborate analysis in the cited papers is a potential source of misinterpretation.

In summary, we propose that the lower- and higher-energy pools of Chls lie on the two opposite sides of RC around the B- and A-branch electron transfer Chls, respectively. These two pools exchange the excitation energy preferentially via two peripheral core antennas but are not able to do this via RC Chls. Thus, our results support the transfer-to-the-trap-limited model and the funneling arrangement of Chls in the PSI core.

Acknowledgments We are thankful to Prof. A. Freiberg for a valuable discussion. This work was supported by the DOE. K.R. acknowledges support from an NSF CAREER award (MCB-0347935). K.G. gratefully acknowledges financial support from the Polish government (scientific project no 1 P03B 003 29).

References

Ben-Shem A, Frolow F, Nelson N (2003) Crystal structure of plant photosystem I. Nature 426:630–635

Bruggemann B, Sznee K, Novoderezhkin V, van Grondelle R, May V (2004) From structure to dynamics: modeling exciton dynamics in the photosynthetic antenna PS1. J Phys Chem B 108:13536–13546

Byrdin M, Jordan P, Krauss N, Fromme P, Stehlik D, Schlodder E (2002) Light harvesting in Photosystem I: modeling based on the 2.5-Å structure of Photosystem I from *Synechococcus elongatus*. Biophys J 83:433–457

Damjanović A, Vaswani HM, Fromme P, Fleming GR (2002) Chlorophyll excitations in Photosystem I of *Synechococcus elongatus*. J Phys Chem B 106:10251–10262

Fromme P, Jordan P, Krauss N (2001) Structure of photosystem I. Biochim Biophys Acta 1507:5–31

Freiberg A, Timpmann K, Lin S, Woodbury NW (1998) Exciton relaxation and transfer in the LH2 antenna network of photosynthetic bacteria. J Phys Chem 102:10974–10982

Gibasiewicz K, Ramesh VM, Melkozernov AN, Lin S, Woodbury NW, Blankenship RE, Webber AN (2001) Excitation dynamics in the core antenna of PS I from *Chlamydomonas reinhardtii* CC2696 at room temperature. J Phys Chem B 105:11498–11506

Gibasiewicz K, Ramesh VM, Lin S, Woodbury NW, Webber AN (2002), Excitation dynamics in eukaryotic PS I from *Chlamydomonas reinhardtii* CC269 at 10 K. Direct detection of the reaction center exciton states. J Phys Chem B 106:6322–6330

Gobets B, van Amerongen H, Monshouwer R, Kruip J, Rögner M, van Grondelle R, Dekker JP (1994) Polarized site-selected fluorescence spectroscopy of isolated photosystem I particles. Biochim Biophys Acta 1188(1994):75–85

Gobets B, van Grondelle R (2001) Energy transfer and trapping in photosystem I. Biochim Biophys Acta 1507:80–99

Gobets B, van Stokkum IHM, van Mourik F, Dekker JP, van Grondelle R (2003) Excitation wavelength dependence of the fluorescence kinetics in Photosystem I particles from *Synechocystis* PCC 6803 and *Synechococcus elongatus*. Biophys J 85(6):3883–3898

Guergova-Kuras M, Boudreaux B, Joliot A, Joliot P, Redding K (2001) Evidence for two active branches for electron transfer in Photosystem I. Proc Natl Acad Sci USA 98:4437–4442

Hastings G, Hoshina S, Webber AN, Blankenship RE (1995) Universality of energy and electron transfer processes in photosystem I. Biochemistry 34:15512–15522

Holzwarth AR, Mu1ller MG, Niklas J, Lubitz W (2005) Charge recombination fluorescence in Photosystem I from *Chlamydomonas reinhardtii*. J Phys Chem B 109:5903–5911

Jordan P, Fromme P, Witt HT, Klukas O, Saenger W, Krauß N (2001) Three-dimensional structure of cyanobacterial photosystem I at 2.5 resolution. Nature 411:909–917

Kleinherenbrink FAM, Hastings G, Wittmershaus B, Blankenship RE (1994) Delayed fluorescence from Fe-S type photosynthetic reaction centers at low redox potential. Biochemistry 33:3096–3105

Klug DR, Giorgi L, Crystal B, Barber J, Porter G (1989) Energy transfer to low energy chlorophyll species prior to trapping by P700 and subsequent electron transfer. Photosynth Res 22:277–284

Krabben L, Schlodder, Jordan R, Carbonera D, Giacometti G, Lee H, Webber AN, Lubitz W (2000) Influence of the axial ligands on the spectral properties of P700 of Photosystem I: a study of site-directed mutants. Biochemistry 39(42):13012–13025

Lee H, Bingham SE and Webber AN (1998) Methods in Enzymology, vol 297. Academic Press, Inc., FL, pp 311–319

Melkozernov AN, Su H, Lin S, Bingham S, Webber AN, Blankenship RE (1997) Specific mutation near the primary donor in Photosystem I from *Chlamydomonas reinhardtii* alters the trapping time and spectroscopic properties of P700. Biochemistry 36:2898–2907

Melkozernov AN, Su H, Webber AN, Blankenship RE (1998) Excitation energy transfer in thylakoid membranes from Chlamydomonas reinhardtii lacking chlorophyll b and with mutant Photosystem I. Photosynth Res 56:197–207

Melkozernov AN, Lin S, Blankenship RE (2000a) Excitation dynamics and heterogeneity of energy equilibration in the core antenna of photosystem I from the cyanobacterium Synechocystis sp. PCC 6803. Biochemistry 39:1489–1498

Melkozernov AN, Lin S, Blankenship RE (2000b) Femtosecond transient spectroscopy and excitonic interactions in Photosystem I. J Phys Chem B 104:1651–1656

Melkozernov AN, Lin S, Blankenship RE, Valkunas L (2001) Spectral inhomogeneity of photosystem I and its influence on excitation equilibration and trapping in the cyanobacterium Synechocystis sp PCC6803 at 77 K. Biophys J 81(2):1144–1154

Müller MG, Niklas J, Lubitz W, Holzwarth AR (2003) Ultrafast transient absorption studies on Photosystem I reaction centers from Chlamydomonas reinhardtii. 1. A new interpretation of the energy trapping and early electron transfer steps in Photosystem I. Biophys J 85:3899–3922

Ramesh VM, Gibasiewicz K, Lin S, Bingham SE, Webber AN (2004) Bi-directional electron transfer in Photosystem I: accumulation of A_0- in A-side or B-side mutants of the axial ligand to chlorophyll A_0. Biochemistry 43(5):1369–1375

Savikhin S, Xu W, Chitnis PR, Struve WS (2000) Ultrafast primary processes in PS I from Synechocystis sp. PCC 6803: Roles of P700 and A_0. Biophys J 79:1573–1586

Savikhin S, Xu W, Martinsson P, Chitnis PR, Struve WS (2001) Kinetics of Charge Separation and A0 $\rightarrow$ A1 Electron transfer in Photosystem I reaction centers. Biochemistry 40:9282–9290

Sener MK, Lu D, Ritz T, Park S, Fromme P, Schulten K (2002) Robustness and optimality of light harvesting in cyanobacterial Photosystem I. J Phys Chem B 106:7948–7960

Shipman LL (1977) Oscillator and dipole strengths for chlorophyll and related molecules. Photochem Photobiol 26:287–292

Valkunas L, Liuolia V, Dekker JP, van Grondelle R (1995) Description of the energy migration and trapping in Photosystem I by a model with 2 distance scaling parameters. Photosynth Res 43:149–154

Van Amerongen H, Valkunas L, van Grondelle R (2000) Photosynthetic excitons. World Scientific, Singapore

Van Stokkum IHM, Larsen DS, van Grondelle R (2004) Global and target analysis of time-resolved spectra. Biochim Biophys Acta 1657:82–104

Webber AN, Gibbs PB, Ward JB, Bingham SE (1993) Site-directed mutagenesis of the Photosystem I reaction center in chloroplasts – the proline-cysteine motif. J Biol Chem 268:12990–12995